RAST Model: simulation of tensiotraces to facilitate drophad engineering

Philippe Pringuet[1], N D McMillan[2], G Doyle[2], S R P Smith[3], M ONeill[4], S Riedel[5]

[1] Bahrain Polytechnic, BP33349, Isa Town, Kingdom of Bahrain
[2] Institute of Technology Carlow, Kilkenny Road, Carlow, Ireland
[3] Physics Department, University of Essex, Wivenhoe Park, Colchester, Essex CO4 3SQ, UK
[4] Carl Stuart Ltd, Whitestown Business Park, Tallaght, Dublin 24, Ireland
[5] Dublin Institute of Technology, Dublin, Ireland

E-mail: `philippe.pringuet@polytechnic.bh`

Abstract.
Tensiography is a technique that determines the physical and chemical properties of a liquid by illuminating a growing pendant drop from within using a source fibre. Light reflected internally at the surface of the drop is recieved by a collector fibre and is converted into an electric signal called a tensiotrace, which is a graph of reflected light as a function of drop volume. The instrument obtaining this signal is called multianalyser. A numerical model that simulates tensiotraces through a raytracing analysis (RAST - Raytracing Analysis for the Simulation of Tensiotraces) of the multianalyser as been developed to define theoretically how the tensiotrace describes the physical and chemical properties of a liquid. The purpose of this study is to investigate the model as an engineering/design assistant leading to discoveries and improvements to the multianalyser.

1. Introduction

1.1. Tensiography

Tensiography [1] is a technique that determines physical and chemical properties of a liquid [2] from illuminating a growing pendant drop from within by a source fibre. Light reflected at the surface of the drop is received by a collector fibre and is converted into an electric signal called a tensiotrace, the graph of reflected light intensity versus drop volume. The tensiotrace records the entire drop history from remnant drop initiations until the mature drop separates. The optical tensiograph [3] (also known as drop analyser or multi analyser) is an Amplitude Modulated Fibre Optic Sensor (AMFOS) instrument that records tensiotraces.

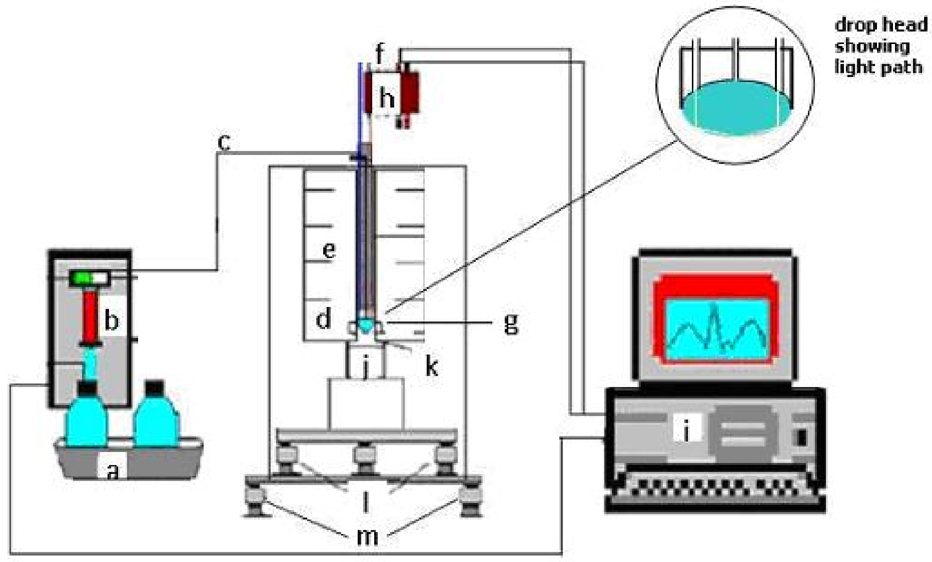

	Description		Description
a	Sample for analysis	h	Detector
b	Stepper-motor-pump	i	Computer
c	Delivery tube	j	Chamber to ensure saturation of atmosphere
d	Drophead	k	Temperature sensors
e	Temperature control	l	Auto levelling drives
f	Light Source	m	Anti vibration balancing feet
g	Optical Eyes		

Figure 1: Schematic diagram of the tensiograph instrument

The scheme of the instrument arrangement is shown in figure 1. The liquid a, which is to be analysed is pumped via the liquid delivery tube c to the drophead d using a motor stepper pump b and a pendant drop grows at a uniform volume rate (isochoric) in size until it separates from the drophead. Throughout this process, light from a light emitting diode (LED) f is injected into the drop through the source-fibre and the reflected signal, picked up by the collector-fibre is transmitted to a photodiode h. The amplification of the low photocurrent into an adequate voltage signal is necessary before the signal is passed to an acquisition board (an electronic system based on a programmable interface controller (PIC) and other suitable electronics hardware) incorporated in a personal computer (PC) i. The Peltier temperature control block e maintains the temperature of the LUT at usually $20°C$ or $25°C 0.1°C$. The optical eyes g enable the signal to be scissored - the initial trigger occurs when the initiation drop falls through the optical eye and triggers the start of the data acquisition, indicating when the measurement drop has arrived on the drophead and then the data acquisition continues until this drop falls off the drophead and the second trigger locates precisely the ending of recording of the tensiotrace (a data set recorded over the life cycle of the drop). Two-stages anti-vibration mounts l and m protect the drop from vibrations. The analogue to digital converter (ADC) of the acquisition board converts the analogue voltage (amplified optoelectronic signal from the detector) into a digital signal, which is then subsequently transferred to the memory of the PC where it is stored for later analysis. There is a source-detector employing a CCD (charged couple device) or CMOS (complementary metal oxide semi-conductor) detector in conjunction with a spectral source such as fibre deuterium, xenon, halogen or tungsten sources. Such a system provides a spectral array of tensiotraces; one for every measurement wavelength.

The instrument has been engineered to deliver measurements of the physical properties of the LUT, namely surface tension/density ratio, refractive index (η), colour at a specific wavelength ($absorption = A_\lambda$) and turbidity at a specific wavelength. The instrument can also be used for quality assurance for solid products such as pharmaceutical products if these are dissolved in an appropriate solvent for this purity/fingerprinting assay. It can also be used to sensitively monitor chemical and biochemical kinematics processes.

Figure 2 shows a typical concave drophead. The practical problem with such a design is fundamental in that physical damage can be caused due to exposure of the fibres. As a result of this study, a patented quartz drophead has been designed that gives the same universal fingerprint capability as this traditional drophead. This new design of drophead is one of the key innovations that facilitates accurate, reproducible and sensitive tensiography. Tensiography has potential to contribute to quality assurance in the wine industry in terms of chemical analysis and fingerprinting.

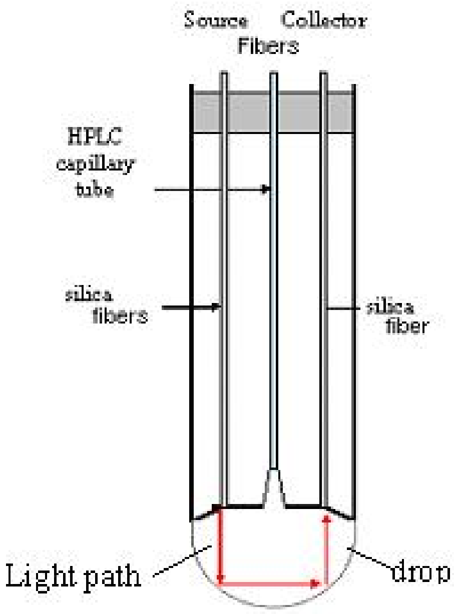

Figure 2: Drophead configuration

1.2. Tensiotraces

The key concept of the tensiograph is the fact that all the various physical and chemical processes that modulate the coupled light in the drop produce a signal, which is unique in

Journal of Physics: Conference Series **307** (2011) 012007 doi:10.1088/1742-6596/307/1/012007

a theoretical sense for every specific combination of properties of the LUT. These processes include (i) partial reflection of the light beam inside the pendant drop, (ii) absorption of the light from chromophores in the liquid, (iii) scattering of the light from turbid particulate matter, (iv) changes in the emission angle from the source fibre, and indeed perhaps other processes. The detected light intensity is amplitude modulated during the life cycle of a drop i.e. the reflecting surface of the inner drop changes continuously. Figure 3 shows the characteristic features of a tensiotrace. The physical features of tensiotraces are defined by the physical and chemical properties of the LUT such as density, colour, refractive index and adbsorbance. Although each of these can be measured from tensiotraces, the measurands are not statistically independant.

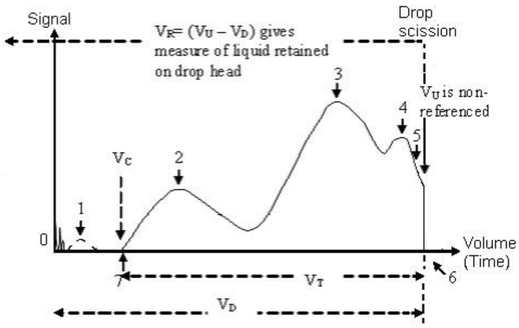

Label	Description
0	Separation vibration
1	First-order peak (protopeak)
2	Rainbow (second-order deuteropeak)
3	Tensiopeak (third-order tritopeak)
4	Shoulder peak (fourth-order tetertopeak)
5	Separation peak (fifth-order pemptopeak)
6	Drop period
7	Rainbow peak commencement

Figure 3: Tensiotrace showing the important trace features associated with drop mechanics, labeled 0 to 7

The first-order peak (proto-peak) is not seen in the current drophead design where the first order coupling is geometrically impossible because the measurement drop is too flat with the widely spaced fibres. The horizontal axis can be either volume or time as both are equivalent for constant volume delivery from stepper pumps. Here only volume is shown but this quantity is derived from a time measurement.

The positioning of the fibres in the drophead has been engineered to optimise the measurement of various physical/chemical properties. The rainbow peak height and position in the tensiotrace is a good measure of refractive index. It gets its name from the fact that in rainbows a measurement of the angle of the bow to that of the observer provides a measurement of the refractive index of the liquid. The height of the major tensiograph peak (3-tensiopeak) provides a good measurand for determining the colour and/or turbidity of the solution in that this decreases with respectively the increasing absorptive or scattering power of the liquids. The drop period can be used to give a good measure of the surface tension/density ratio. Other physical measurements have been shown to be possible with the tensiograph, but the principal use of the tensiograph is as a fingerprinting technique. The combination of the physical and chemical properties of the drop defines the form of the tensiotrace and thus the tensiotrace provides a very sensitive fingerprint technique for liquids, or indeed solid samples dissolved in a solvent.

The computer model described below reveals that the coupling of the light from source fibre to collector fibre can be represented as a 2-D process as the drop grows and with this volume growth higher reflection orders develop. The light must enter the collector fibre within the acceptance angle. Therefore the first order 'single' reflection off a position close to the centre of the drop base in the smallest drop does not couple to the detector. An important measurement position is known as the commencement or RPC (7 in figure 1) at which the light from source fibre is received by the collector fibre and can be transmitted in the multimode fibre to the detector. In the drophead design used in this study no light couples to the detector until the second order reflection begins to develop in a larger drop with reflections off either side of the drop.

1.3. The RAST model

A computer program that simulates tensiotraces through a raytracing analysis (RAST model) has been developed using Matlab to define the formation of tensiotraces. Modeled tensiotraces from this model were compared qualitatively and quantitatively to experimental tensiotraces of different liquids in order to evaluate the model.

A representation of the drophead is coded in the program. All dimensions including indent of the quartz disc, position and size of the fibres are normalised on the radius of the drophead. This is the basis of a dimensionless invariant model. Figure 4 shows a 2D cross section of the drophead model; notice the scale is normalised to -1 ... 1. The drop head dimensions are extremely important for the model and are later used when simulating the rays of light.

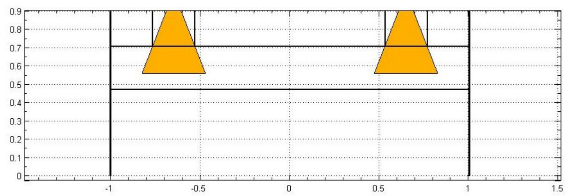

Figure 4: Representation of a drophead

In this schematic representation of the quartz drop head (figure 4), the quartz disc protecting the fibres is clearly visible. The two vertical lines on the outside of the disc represent the edges of the lip and the two small rectangles at the top are the fibers. The emitting fiber cone of light and the detector fiber acceptance angle are represented by the triangles. This representation is only an approximation since these dimensions can only be fabricated by Starna with a tolerance of 0.1 mm. In particular the edge of the drophead cannot be fabricated as represented.

The RAST model is best described by figure 5. Each drop shape is grown incrementally from the apex using Runge-Kunta 4 algorithms and following the Laplace-Young equation until the radius of the drop shape is 1 (normalised drophead diameter = 2).

The life cycle of the drop is created by modelling the drop shapes from the value of X_0 that corresponds to the solution with the smallest permissible volume. Solutions for smaller drop shapes could be obtained but the corresponding drop would not attach to the drophead edge (angle of attachment too small) and as such would be smaller than the remnant drop. X_0 is then increased incrementally and more drop shapes are calculated. A point is eventually reached when a further increase in X_0 actually results in a decrease in volume. This point in the drop cycle is considered to be the theoretical drop separation. Indeed, as more liquid is pumped in the drop, the drop has to increase in size or fall. Since there is no more solution to the equation forming a larger drop, the drop must have fallen. This is a theoretical maximum and it is believed that the drop separation can be slightly earlier as vibrations and liquid fluid mechanics are not taken in consideration here.

To form a tensiotrace, light emitted from the fibre goes through the drop and is coupled to the detector fiber. The model follows the same principle, modelling the light as a collection of rays. The emission from the multimode fibre is modelled by a cone of rays from the source fiber

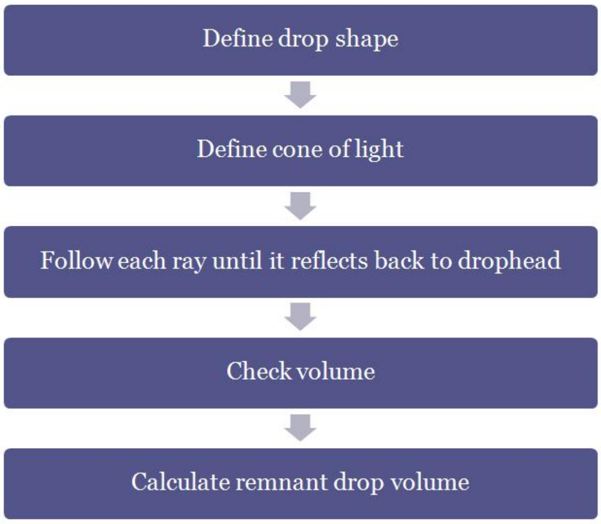

Figure 5: RAST algorithm

comprising at least 1000 rays (100,000 is more typical). Each ray starts from the surface of the fiber and has a direction limited by the numerical aperture of the fiber. This collection of rays forms the cone of light previously mentioned. Figure 4 shows the cone of light given by the numerical aperture of the fibers. In order to cover the fibre end uniformly, a parameter n_{th} is defined, corresponding to the number of possible values of theta (angle of ray with vertical norm) between 0 and the numerical aperture NA. $n_{th} = 200$ corresponds to 125830 rays calculated per dropshape and is the value used for data collection. The emission from a fibre is non-uniform and the intensity is accurately described by a $cos\theta$ function [4] based on the Warn's illumination model [5].

Rays first have to go through the quartz disc protecting the fibre from the liquid. Light is refracted at each interface and the new direction is calculated using the Fresnel equation [6]. Similarly to the emission end, rays when reaching the quartz disc are refracted on to the fibres level. The position is calculated as well as the angle of incidence. Rays are coupled (transmitted along the fiber and reach the detector) only if they hit the collector fiber with an incidence angle less or equal to the numerical aperture of the fiber. If the ray is coupled to the detector fiber, its intensity is added to the tensiotrace intensity for that volume.

2. Experimental

The testing involves the engineering process to create the new patented quartz drop head (see figure 6) made by Starna and the repercussions on the measurement capabilities of the instrument. The main objective is to show how the model can be used to improve the drophead design for a particular application. Each set of result gives a better understanding of tensiography and the tensiotraces. Also testing a new drophead design in order to obtain the desired tensiotrace can be very costly both financially and in man-hours. Indeed it requires changing the design and building a new prototype but also retesting the new drophead and analysing the results. The model facilitates this analysis at a fraction of the cost.

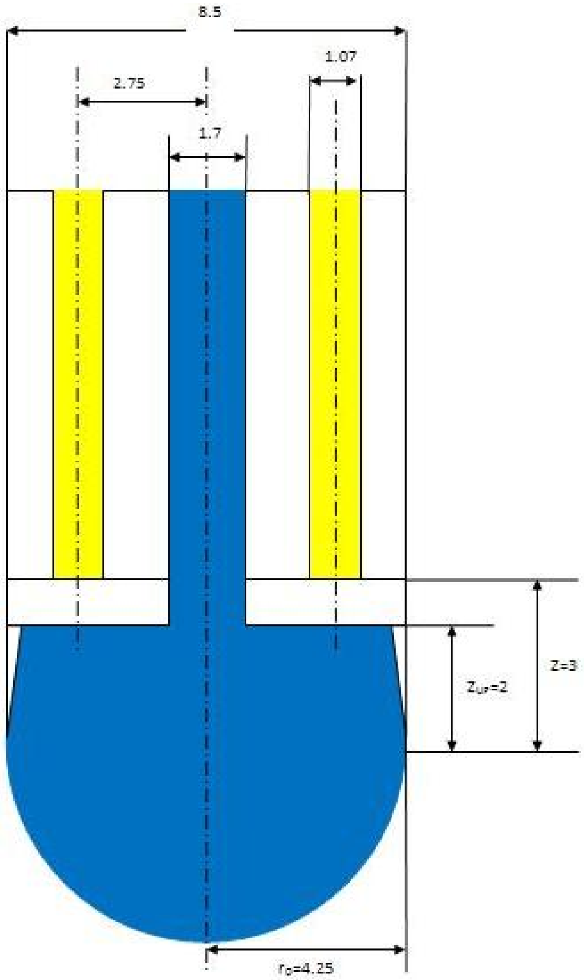

Figure 6: Representation of the quartz drophead

Simulations have been carried out in order to test the effect of different measurements of the new quartz drophead.

- the disc thickness
- the fibre diameter
- the fibre position
- the edge height (Z_{UP})

A cross section analysis was also carried out in order to study the impact position of rays and evaluate the possibility of simultaneous multi-wavelength analysis.

3. Results

3.1. Analysis of the disc thickness

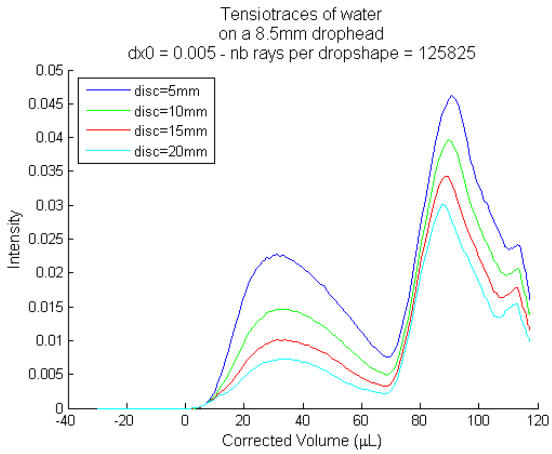

Figure 7: Modeled Tensiotraces of water for various disc thickness

Figure 7 shows the effect of the size of the quartz disc on tensiotraces. Although quartz is a transparent medium, the thicker the disc, the less light goes through; this results in lowering the intensity of the tensiotrace. It should be noted that the quartz disc is protecting the fibres from the LUT and the possible damages from proteins **??**. Another effect of the quartz disc is to narrow the numerical aperture of the fibres as the refractive index of the disc is different from the refractive index of the fibres. This is shown by a larger reduction of intensity on the rainbow peak than on the tensio peak. This is shown in figure 8 where the downward slope for RPH is greater than for TPH. Ideally the smaller thickness is preferred as optical coupling is optimised but fabrication issues force the minimum size to 1mm.

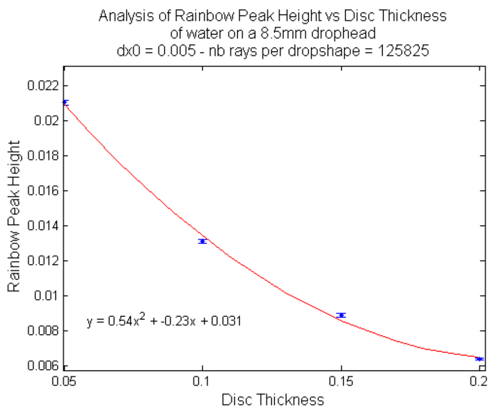

(a) Rainbow Peak Height

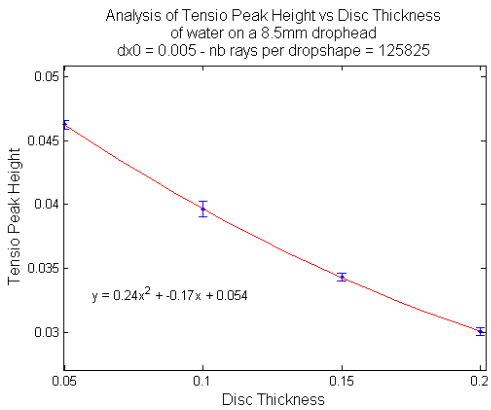

(b) Tensio Peak Height

Figure 8: Analysis of effect of disc thickness on RPH and TPH

3.2. Analysis of the fibre diameter

Figure 9 shows the effect on tensiotraces when changing the diameter of both fibres. Even though the simulations could have been carried out with input and output fibres of different diameter,

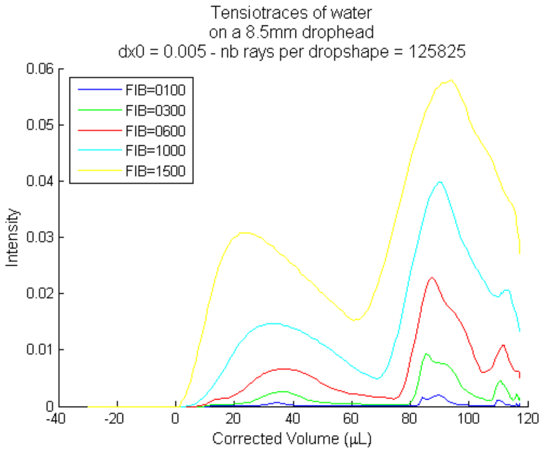

Figure 9: Modeled tensiotraces of water for various fibre diameters

this would cause problems when fabricating the drop heads as drilling quartz is a challenging process. The different fibres simulated were taken from the artphotonics catalogue [7].

Increasing the diameter of the fibres effectively increases the light being transmitted to the detector and as such probably increases the detection limit. In drop spectroscopy good quantitative capability is required. It is achieved by maximising the optical throughput (i.e. increasing the fibre diameter). However, the drophead was designed in order to maximize the resolution of each peak. The larger fibre simulated here ($FIB = 1500\mu m$) affects the quality of the tensio peak to such a degree that the shoulder peak disappears. It can be argued that 600 micron fibres give a better resolution of separation peak and noticeably better symmetry in the rainbow peak. In practice, a compromise is found using 1000 micron fibres but this does not seem to be the best option in all cases. It is important that the drop head is designed for purpose. The RAST model can help achieve this. Figure 10 shows that the fibre diameter has a linear relationship with the tensiopeak height.

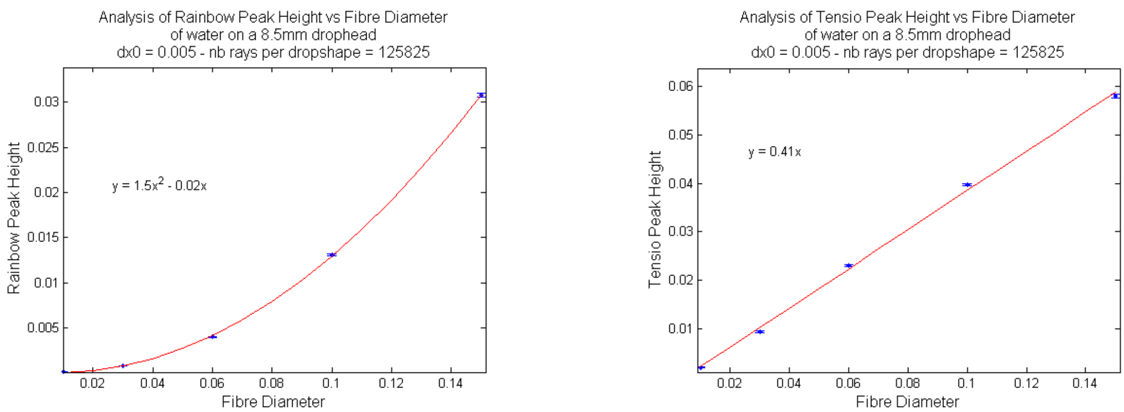

(a) Rainbow Peak Height

(b) Tensio Peak Height

Figure 10: Analysis of effect of fibre diameter on RPH and TPH

3.3. Analysis of fibre position

Tensiotraces of water were modelled on a quartz drophead with different positions for centre of the input and output fibres between 2.5 and 3.5mm from the centre of the drophead.

The relation between Rainbow Peak Commencement and Remnant Drop Volume was first analysed to make sure that the full tensiotrace could be recorded on the multianalyser ($RPC < 0$ result in the start of the rainbow peak not being recorded). The definition of the peak was also rated from poor to good in order to discard poorly defined tensiotraces. It was concluded that symmetric position of the fibres often give better defined peaks. Also fibres cannot be placed too close to the edge of the drophead (3.25mm and 3.5mm from centre) to avoid problems with the start of the rainbow peak or fabrication. A symmetric design of the drophead is also an advantage in the construction stage.

Peak heights were then analysed (see figure 11) in order to find the tensiotrace with the best throughput. It should be noted that the tensiotraces from drophead B and C and from drophead E and F are identical because it does not matter which fibre is connected to the source and which is connected to the detector.

Test Nb	Position of fibres source	detector	Peaks analysis RPH	TPH	RP symmetry	SP definition
A	2.50mm	2.50mm	0.0063	0.0365	good	good
B	2.50mm	2.75mm	0.0080	0.0345	good	poor
C	2.75mm	2.50mm	0.0080	0.0345	good	poor
D	2.75mm	2.75mm	0.0146	0.0397	average	good
E	2.75mm	3.00mm	0.0189	0.0383	good	poor
F	3.00mm	2.75mm	0.0189	0.0383	good	poor
G	3.00mm	3.00mm	0.0340	0.0440	poor	average

Table 1: Analysis of water tensiotraces peaks for various fibre positions

Test A gives a tensiotrace of lesser quality with a very flat (although very symmetrical) rainbow peak which may cause accuracy problems when calculating apex coordinates. Visual inspection reveals that the best position for the fibres seems to be symmetrical 3mm from the centre although the rainbow peak is not well balanced. Current version of the quartz drophead (Test D - symmetrical 2.75mm from the centre) gives a well defined tensiotrace with arguably a better balanced and more symmetric rainbow peak but with a smaller throughput. However water is at the bottom of the RI range. A low RPH for water gives a greater dynamic range for RI. Hence this choice of fibre position is best overall.

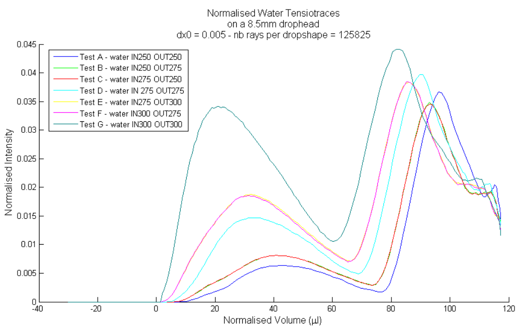

Figure 11: Analysis of water tensiotraces for various fibre positions

3.4. Analysis of Z_{UP}

The Z_{UP} dimension corresponds to the width of the protruding edges on the drophead (see figure 6). $Z_{UP} = 0$ corresponds to a flat drophead. Increasing Z_{UP} has a similar effect to increasing the disc thickness with the overall intensity of the drophead decreasing as well as the numerical aperture. It also has a strong effect on the tensiopeak, especially in the case of coloured LUT. Increasing Z_{UP} also increases the path length of the rays in the liquid, decreasing the tensiopeak height in a similar way to absorbance.

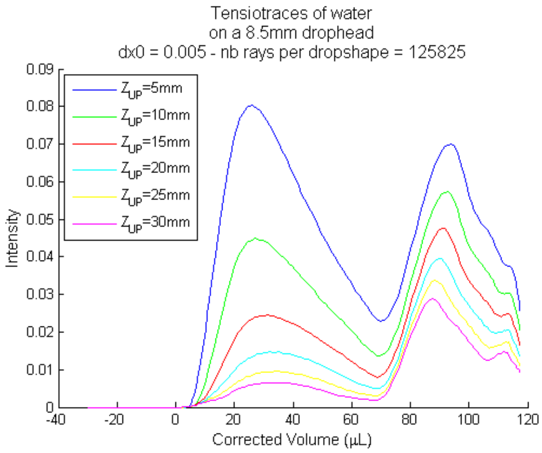

Figure 12: Modeled tensiotraces of water for various lip height

The modelling (see figure 12) shows the result of using a 2mm design is compromised as this is about 10 times poorer than the 0mm head. However, these protruding edges are necessary. It was designed to counter the wetting problem encountered with the first design of the quartz drophead and stop liquids with high surface tension to leak onto the upper edge of the drophead. This practical problem is one that stops proper measurement. Although $Z_{UP} = 0$ gives the best result it is not a practical option as there is no lip. Starna's engineering capability is pushed to the limit with small values and they cannot make them reproducibly with values of less than 2mm. Figure 13 shows the lip height has a greater effect on RPH because it increasing the lip height has a similar effect as changing the numerical aperture of the fibres.

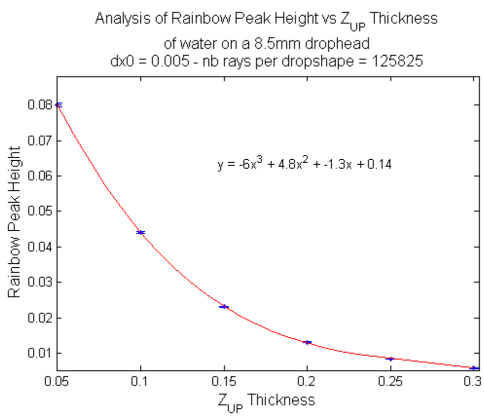

(a) Rainbow Peak Height

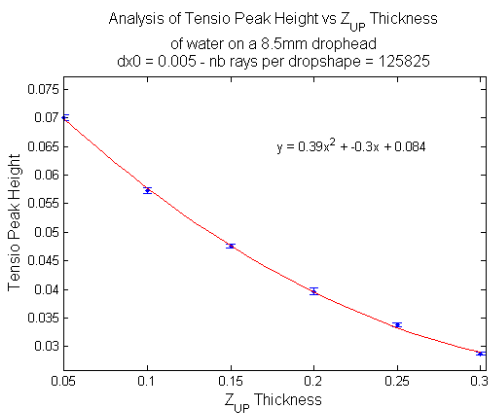

(b) Tensio Peak Height

Figure 13: Analysis of effect of lip height on RPH and TPH

3.5. Cross section analysis

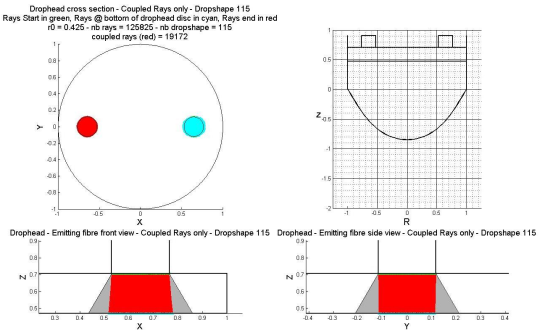

Figure 14: Drop head cross section analysis of coupled rays at Rainbow Peak

3.5.1. Analysis of coupled rays Top left corner of figure 14 shows a cross section view of the drophead and the coupled rays for the rainbow peak. As described above input rays cover uniformly the input fibre (right fibre). The detector fibre (left fibre) also makes full use of fibre end to collect light. The insert graphs at bottom respectively show a front view (bottom left insert) and side view (bottom right insert) of the input fibre. Only coupled rays are shown. Left insert reveals that although light is shining in every direction (within the aperture), only rays shining approximately vertically find their way to the detector fibre. Also, only **75%** of the cone of light is coupled, confirming the choice of fibre to be adequate. This is even more true in the side view of the emitting fibre.

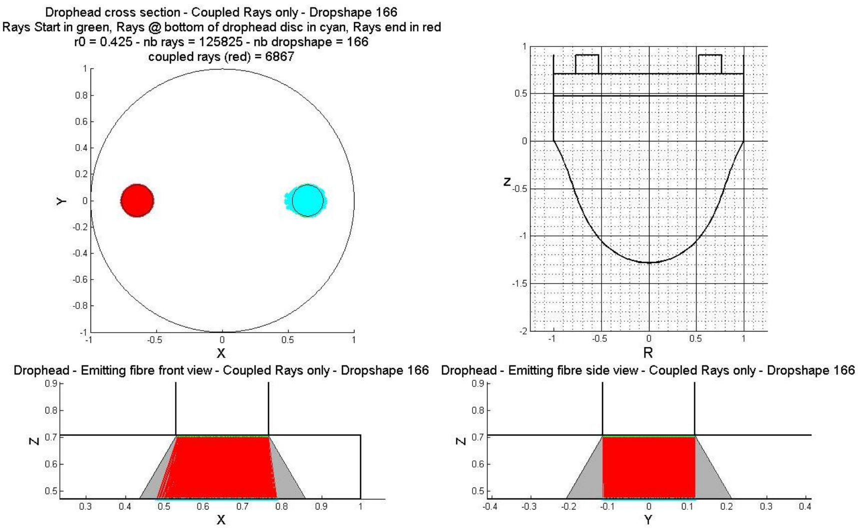

Figure 15: Drop head cross section analysis of coupled rays at Tensio Peak

Analysis of the coupled rays for the tensiopeak (see figure 15) and at the drop period (see figure 16) revealed the same conclusions as for the rainbow peak even though drop shapes are radically different. This confirms that positioning of the fibres, disc thickness and edge width are essential design features and are here optimised with regards to fabrication capabilities.

Analysis of the rainbow peak commencement (see figure 17) confirms experimental results that RPC is bound to the geometry of the drop and the drophead design, i.e. spacing between fibres.

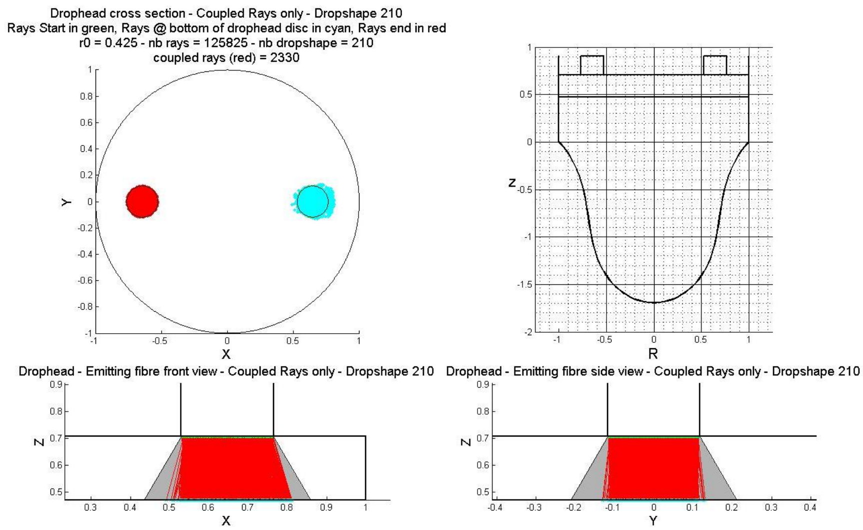

Figure 16: Drop head cross section analysis of coupled rays at Drop Period

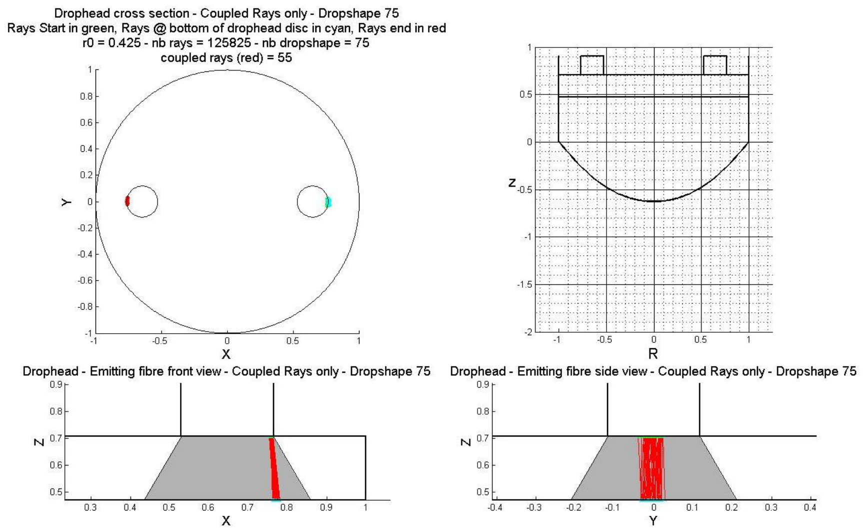

Figure 17: Drop head cross section analysis of coupled rays at Rainbow Peak Commencement

3.5.2. Analysis of lost rays Analysis of non coupled rays (lost rays) can help predict the potential of a design change, especially in regards to fibres diameter and position.

Figure 18 shows impacts of rays that did not reach the detector for the rainbow peak. They are not coming from a particular area of the input fibre nor a particular angle. However, most (**over 50%**) seem to hit the bottom of the drophead within the vicinity (within 2mm) of the detector fibre. This leads to the conclusion that a wider detector fibre (=2mm) would increase the overall intensity of the tensiotrace thus increasing the detection limit. However it might have a negative effect on the definition of peaks. Also, with it being a difficult process to drill accurately into quartz, in order to keep costs down it is a prerequisite to have both fibres of the same diameter. As with coupled rays, it is shown here that rays converge towards the detector fibre due the concave shape of the drop. It is then possible to add one or two pairs of fibres inside

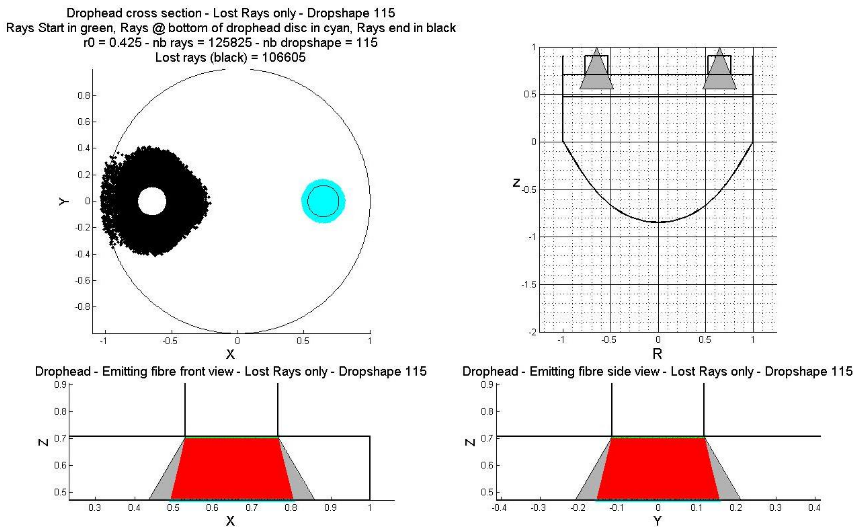

Figure 18: Drop head cross section analysis of non coupled rays at Rainbow Peak

the drophead in order to simultaneously analyse the LUT using different wavelength. Rays of different fibres would not affect each other.

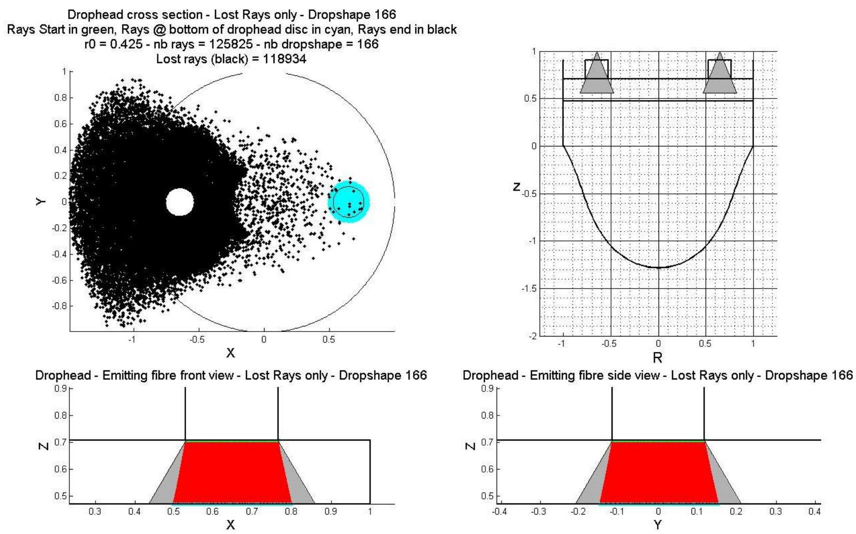

Figure 19: Drop head cross section analysis of non coupled rays at Tensio Peak

Rays that did not couple at the tensiopeak however do not converge toward the detector fibre but seem to cover a wider area thus reducing the possibility of simultaneous analysis using multiple fibre pairs (see figure 19).

Journal of Physics: Conference Series **307** (2011) 012007 doi:10.1088/1742-6596/307/1/012007

4. Conclusion

This paper shows that theoretical testing was crucial to create the new patented quartz drop head and explains design choices and their repercussions on the measurement capabilities of the instrument. The main objective (to show how the model can be used to improve the drophead design for a particular application) was achieved at a fraction of the normal cost. The RAST model allows to design the drophead to fit the purpose but in practice there has to be some compromises with Starna's engineering capability.

References

[1] McMillan N D 1988 Method and apparatus for analysing liquid properties.
[2] McMillan N 1993 *Opto-Laser Europe* 42–43
[3] McMilllan N, Lawlor V, Baker M and Smith S 1998 *Drops and Bubbles in Interfacial research* **6** 593–705
[4] Adams M 2000 Fibre emission cone itensity
[5] Wernert E A 2002 Interactive computer graphics lectures - lighting and shading models
[6] Hecht E 2002 *Optics* 4th ed (San Francisco ; London : Addison-Wesley , c2002.)
[7] Artphotonics 2008 Uv - sillica fibers `http://www.artphotonics.de/SIF/002/index.php`